Tellus
SERIES B
CHEMICAL
AND PHYSICAL
METEOROLOGY
PUBLISHED BY THE INTERNATIONAL METEOROLOGICAL INSTITUTE IN STOCKHOLM

Tellus (2009), 61B, 408–415
Printed in Singapore. All rights reserved

TELLUS

Variations of atmospheric nitrous oxide concentration in the northern and western Pacific

By K. ISHIJIMA[1,*], T. NAKAZAWA[2] and S. AOKI[2,1] *Frontier Research Center for Global Change/JAMSTEC, Yokohama 236–0001, Japan;* [2] *Center for Atmospheric and Oceanic Studies, Tohoku University, Sendai 980–8578, Japan*

(Manuscript received 22 February 2008; in final form 21 October 2008)

ABSTRACT

Atmospheric N_2O concentration was observed in the Pacific for the period 1991–2006, using commercial container ships sailing between Japan and North America and between Japan and Australia or New Zealand. The N_2O concentration showed a secular increase and interannual variations at all sampling locations, but a seasonal cycle was detectable only at northern high latitudes. The annual mean N_2O concentration showed little longitudinal variations (within $\pm$ 0.3 ppb) in the northern Pacific, but showed a clear north-south gradient of about 0.8 ppb, with higher values in the Northern Hemisphere. The annual mean N_2O was also characterized by especially high values at 30°N due to strong local N_2O emissions and by a steep latitudinal decrease from the equator to 20°S due to the suppression of interhemispheric exchange of air by the South Pacific Convergence Zone. The N_2O growth rate showed an interannual variation with a period of about 3 yr (high-values in 1999 and 2000), with a delayed eastward and poleward phase propagation in the northern and western Pacific, respectively. The interannual variations of the N_2O growth rate and soil water showed a good correlation, suggesting that the N_2O emission from soils have an important causative role in the atmospheric N_2O variation.

1. Introduction

Nitrous oxide (N_2O) is one of the Kyoto Protocol greenhouse gases and is also related to the ozone depletion through production of nitrogen oxides in the stratosphere (Forster et al., 2007). Atmospheric N_2O concentration increased considerably from pre-industrial levels of less than 280 ppb to about 320 ppb in 2006, mainly due to the agricultural N_2O emissions (Machida et al., 1995; Flückiger et al., 1999; MacFarling Meure et al., 2006). Systematic measurements of atmospheric N_2O (Weiss, 1981) revealed that the concentration has increased at a growth rate of around 0.7–0.8 ppb yr^{-1} for the last three decades (Prinn et al., 2000; Forster et al., 2007; Ishijima et al., 2007). The growth of global warming potential since 2000 by the N_2O concentration increase is thought to be the second largest, following CO_2 (Hofmann et al., 2006; Forster et al., 2007). This requires a careful evaluation of surface N_2O emissions on a global scale, necessitating an accurate understanding of the temporal–spatial variations of the atmospheric N_2O concentration over a wide geographical area.

Recently, Hirsch et al. (2006) estimated for the first time the N_2O fluxes on the earth's surface by inverse modelling, and they found that the Northern Hemispheric N_2O emission is 1.9–5.2 times more than the Southern Hemispheric emission, which is much higher than the upper limit of previous estimates. Although the large uncertainty in their emission estimation came mainly from the influence of stratospheric N_2O, spatially denser measurements of atmospheric N_2O would also reduce the uncertainty, as was the case in the CO_2 inverse calculations (Gloor et al., 2000; Patra et al., 2003). Furthermore, incorporation of long-term records of N_2O in inverse modelling would be helpful.

To obtain spatially extensive and dense and relatively long records of atmospheric N_2O, we conducted a systematic measurement of atmospheric N_2O in the northern and western Pacific since 1991, utilizing commercial container ships between Japan and North America and between Japan and Australia or New Zealand.

In this paper, we show the results obtained from our shipboard measurements of the N_2O concentration in the Pacific for 14 yr from 1992 to 2005 and discuss temporal and spatial variations of atmospheric N_2O on a hemispheric scale.

2. Procedures of air sampling and N_2O concentration analysis

Air samples have been collected onboard commercial container ships sailing in the northern and western parts of the Pacific Ocean since September 1991. On cruises that took around

*Corresponding author.
e-mail: ishijima@jamstec.go.jp
DOI: 10.1111/j.1600-0889.2008.00406.x

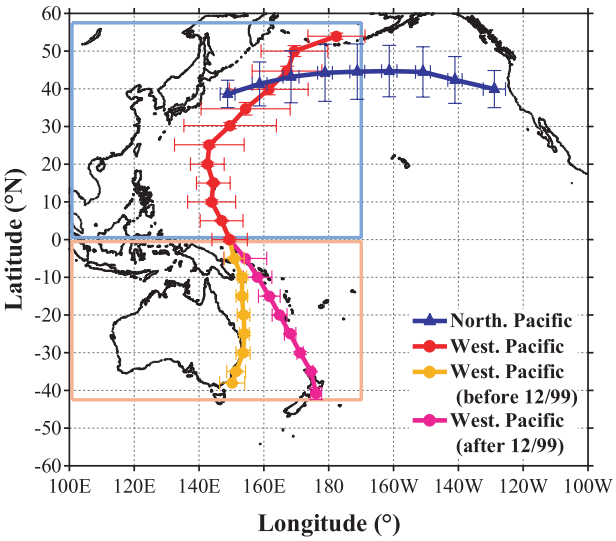

Fig. 1. Locations of air sampling made using commercial container ships in the northern and western Pacific. Each solid mark and its horizontal or vertical bar represent the average location of air sampling and its longitudinal or latitudinal range, respectively. Air sampling in the Southern Hemisphere was made between Japan and Australia before and between Japan and New Zealand after December 1999.

30-day round trip between Japan and North America, covering a region 35°N to 55°N in the North Pacific, about 20 air samples were collected at every 10° between 150°E and 130°W. On the other hand, 30–36 air samples were collected at every 5° between 33°N and 40°S during each of the 40-day round cruise between Japan and Australia (or New Zealand after December 1999). The cruise tracks of the container ships are shown in Fig. 1. The air intake was installed on a windward side of the bridge of the ship to prevent ship contamination, and each air sample was pressurized into a 550 mL Pyrex glass flask with Nitrile O-ring seal to about 0.12 MPa by using an electric diaphragm pump. Before air sampling, all glass flasks were washed by using an ultrasonic cleaner and then evacuated to 1.3 Pa at 100 °C for 6 h.

The N_2O concentrations of the air samples were determined at Tohoku University against our air-based N_2O working standard gases, using a gas chromatograph (GC) equipped with an electron capture detector (ECD). Two sets of GC system were used for this study. The old GC, GC-14A (Shimazu, Japan), was used for the period of October 1991 to December 2002 but was replaced by a new one, Agilent 6890 (Agilent Technologies, USA), in September 2002. By doing so, our measurement precision improved from ±1.0 to ±0.2 ppb. A mixture of highly pure Ar (95%) and CH_4 (5%) was used as a carrier gas for both GC systems. To obtain sufficiently large chromatogram area of N_2O, a 10 mL sample loop was used. The sample air was dried by passing it through a H_2O trap cooled to –80°C before introduction into the sample loop. The sample air introduced into the loop was kept for 30 s to equalize its temperature to that of the oven and then led to the columns. Both GC systems have one precut and two main Porapak columns, and CO_2 and SF_6 contained in the samples were completely separated from N_2O by these columns, so that the respective components of CO_2, N_2O and SF_6 arrive at the ECD in 5.3, 6.9 and 8.7 minutes after introducing the sample air into the precut column. It took about 12 minutes to analyse one air sample on both GC systems. The N_2O concentration values of our working standard gases were 257.75, 306.05 and 350.87 ppb for the old GC system and 121.66, 283.95, 321.08 and 370.17 ppb for the new GC system, which were calibrated against our gravimetrically prepared primary standard gases (Machida et al., 1995). The calibration of the working standard gases against the primary standards was made almost bi-yearly, and no significant concentration differences between the working and primary standards were found. We also examined the possibility of deterioration of air samples during their storage by analysing, for different periods, the N_2O concentration of dried natural air in flasks filled at the same pressure as the air samples. It was found that the N_2O concentration decreased by only 0.1 ppb after 2 months. Therefore, we applied no correction to the measured values of the N_2O concentration in this study. Our GC systems and N_2O concentration analyses were described in detail in Ishijima et al. (2001, 2007).

3. Data analysis

From September 1991 to April 2006, about 2400 and 3800 air samples were collected in the northern and western Pacific, respectively. Data showing anomalous N_2O concentration values due to failure in air sampling and concentration analysis were removed. Measurements taken every 10° between 150°E and 130°W in the northern Pacific were grouped into nine 10° longitude intervals and were used to examine the longitudinal variation in the N_2O concentration. This constituted the North Pacific data set. For the latitudinal variation in the western Pacific, we used the measurements taken every 5° between 30°N and 40°S during cruises between Japan and Australia (before December 1999) and New Zealand (after December 1999). This constituted the Western Pacific data set. We also grouped the data obtained over the western sector (150°E–175°W, 35°N–55°N) of the Japan–North America cruises into five 5° latitude intervals and incorporated them into the Western Pacific data set. Thus, we ended up with a total of 2200 (North Pacific data set) and 4300 (Western Pacific data set) data values (These data are available from the World Data Center for Greenhouse Gases; http://gaw.kishou.go.jp/wdcgg/).

Next, we applied the digital filtering technique by Nakazawa et al. (1997) to extract long-term trends, interannual variations and seasonal cycles. The cut-off period was set to 36 months to derive long-term trends and interannual variations. The average seasonal cycle of the N_2O concentration was approximated by the sum of the fundamental, its first and second harmonics with

the respective periods of 12, 6 and 4 months. The signals with the periods of 4 to 36 months were regarded as irregular variations. The best-fit curve was obtained by summing the long-term trend, the average seasonal cycle and the irregular variations. Any data lying outside ±3 standard deviations were regarded as outliers and excluded from the record. These outlier values were likely a result of contamination by ship and other activities that were not of background nature. This procedure was repeated until no outliers were identified. About 12% of the North Pacific and 11% of the Western Pacific data sets were rejected as outliers by this method. Figure 1 shows average sampling locations and their spatial deviations. The spatial variation of the sampling location is larger in the Northern Hemisphere than in the Southern Hemisphere because ships often changed their courses to avoid severe weather conditions such as typhoon, intense low-pressure systems and strong seasonally prevailing winds in the North Pacific.

We estimated possible errors of the calculated seasonal cycle and the growth rate due to the imprecision of our GC-systems, that is, 1 ppb for the old system and 0.2 ppb for the new system. We randomly introduced the GC imprecision into the measured N_2O concentration values and derived the seasonal cycle and the growth rate by using the above-mentioned analytical method. These procedures were repeated 1000 times, and the standard deviations of the growth rate were found to be about 0.2 and 0.1 ppb yr^{-1} for the old and the new GC systems, respectively, whereas the standard deviation of the seasonal cycle was found to be 0.04 ppb. Errors transferred to the correlation coefficients between the growth rate and the climate factors to be discussed below were about 0.1. These errors are not significant to impact our discussion below.

4. Results and discussion

The observed concentrations of atmospheric N_2O at selected longitudes and latitudes in the northern and western Pacific are plotted in Fig. 2, together with their best-fit curves and long-term trends. Secularly increasing trends, as well as interannual variations are clearly seen, but seasonal cycles are less evident. We also note that the scatter in the data decreases after 2003; this is due to the use of the new GC system beginning from December 2002. The average N_2O growth rates for the period of January 1992 to December 2005 at the nine longitudes in the northern Pacific and the 20 latitudes in the western Pacific were calculated by applying a linear regression to the best-fit curve derived at each of the locations. It is found that the average growth rate is spatially invariant, and that the N_2O concentration increased at about the same rate all over the Pacific, at least for the period of our study. The average growth rates are found to be 0.75 ± 0.01 and 0.74 ± 0.02 ppb yr^{-1} for the northern and western Pacific, respectively. The latter value is weighted for the area between 55°N and 40°S. More details of the temporal N_2O variations are presented later.

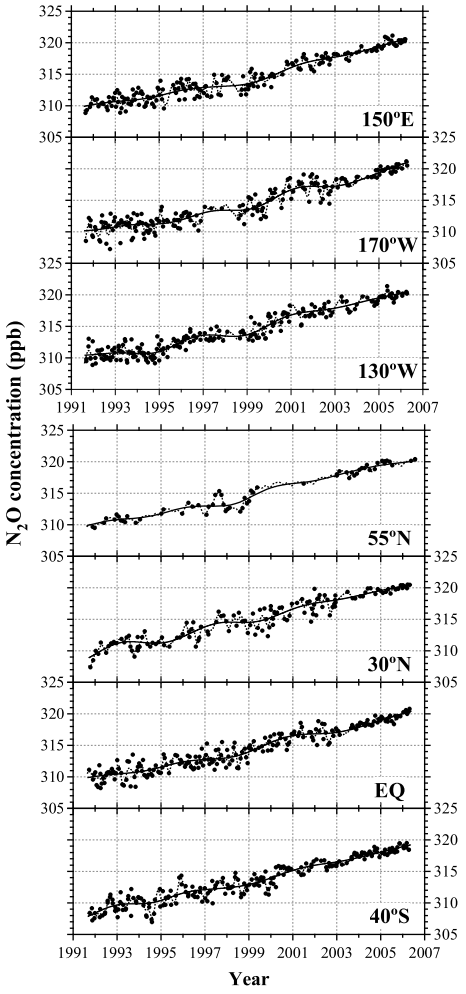

Fig. 2. Atmospheric N_2O concentrations observed at selected longitudes and latitudes in the Pacific. Dots, dashed line and solid line in each panel represent the observed data, their best-fit curve and the long-term trend, respectively.

The annual mean N_2O concentrations are plotted against longitude (northern Pacific) and latitude (western Pacific) in Fig. 3, together with the average values over the period 1992–2005. These annual means were calculated from the long-term trends shown in Fig. 2. Mean standard deviations of the data from the long-term trends are about 1.0, 1.2 and 0.5 ppb for the whole period before and after December 2002, respectively. Figure 3 shows that the annual mean N_2O concentration is nearly uniformly distributed in the east-west direction, with a longitudinal variation of about ±0.3 ppb, which is comparable to our measurement precision. This is a result of zonally well-mixed atmosphere with strong westerlies, in the presence of no strong N_2O sources and sinks.

The latitudinal distribution of the annual mean N_2O concentration shows a north-to-south decreasing value, indicating a stronger N_2O emission in the Northern Hemisphere

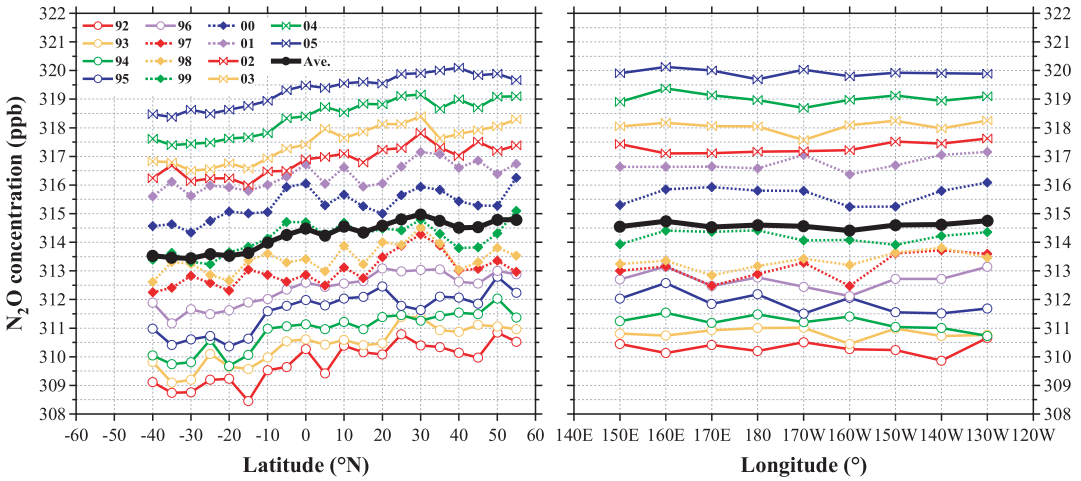

Fig. 3. Latitudinal (left-hand panel) and longitudinal (right-hand panel) distributions of the annual mean N_2O concentration observed in the western and northern Pacific, respectively, for the period 1992–2005. The average distributions for 14 yr are also shown by the black lines.

than in the Southern Hemisphere. The mean interhemispheric difference of the N_2O concentration over the western Pacific for the period 1992–2005 is 0.8 ± 0.2 ppb, similar to the value reported in Ehhalt et al. (2001). By performing a 2-box model calculation (Butler et al., 1989) with the assumptions that the lifetime of atmospheric N_2O is 114 yr (Ehhalt et al., 2001; Forster et al., 2007), the interhemispheric exchange time is 1 yr and both hemispheric total air masses are equal, we estimated the Northern/Southern Hemispheric N_2O emission ratio to be 1.6 ± 0.2 for the period 1992–2005. This ratio is almost the same as Global Emissions Inventory Activity (GEIA; http://www.geiacenter.org/) and Emission Database for Global Atmospheric Research (EDGAR; http://www.rivm.nl/edgar/model/) N_2O inventories yield. On the other hand, Hirsch et al. (2006) obtained the ratios of 1.9–5.2 for the period 1998–2001, which are much higher than the above values, as well as our estimate of 1.4 obtained for the same period. Such a large difference is mainly due to the influence of stratospheric N_2O, which is not considered in our estimation. Hirsch et al. (2006) also mentioned in their paper that the Northern/Southern Hemispheric N_2O emission ratios of over 4, which were obtained under the assumption that the stratosphere–troposphere N_2O exchange in the Northern Hemisphere is twice as large as that in the Southern Hemisphere, are unrealistic. If this is the case, then their estimation decreases to 1.9–2.7, which are closer to ours, but differences between both estimations are still discernible, possibly due to the different observation areas and model parameters such as the interhemispheric exchange time. Strong N_2O emission in the Northern Hemisphere results from the fact that the land area, including both natural and arable soils, is much larger in the Northern Hemisphere than in the Southern Hemisphere, consistent with the idea that N_2O emissions are generally stronger from soils than from the oceans.

We can also see from Fig. 3 that the average latitudinal N_2O distribution shows high values around 30°N. The cause is probably attributable to strong anthropogenic N_2O emissions in the Eurasian Continent and Japan, mainly from agricultural and industrial activities in eastern Asia (Bouwman and Taylor, 1996; Mosier et al., 1998). N_2O emissions from the Pacific Ocean off the east coast of Japan could also contribute to the high N_2O concentrations (Nevison et al., 1995; Suntharalingam and Sarmiento, 2000). Another feature of the average latitudinal N_2O distribution is a steep southward concentration decrease of about 1 ppb between the equator and 20°S. This is caused by the suppression of the southward transport of Northern Hemispheric N_2O due to the South Pacific Convergence Zone (SPCZ), which was usually located around 10°S during our ship cruises.

The National Oceanic and Atmospheric Administration/Earth System Research Laboratory/Global Monitoring Division/Carbon Cycle Greenhouse Gases Group (NOAA/ESRL/GMD/CCGG) also measures N_2O concentration in the Pacific Ocean area. We compared our average latitudinal N_2O distribution for the period 2003–2005 with that from their shipboard measurements between North America and New Zealand, as well as from measurement sites such as Cold Bay, Shemya Island, Sand Island, Guam Island, Cape Kumukahi, Christmas Island, Tutuila Island, Ester Island and Cape Grim (Ed Dlugokencky, personal communication, 2008). By comparing mean N_2O concentrations for the 3 yr at Shemya Island (53°N, 174°E) and Guam Island (13°N, 145°E) to our results at 170°E in the northern Pacific and at 15°N in the western Pacific, respectively, we found that the CCGG values are slightly higher than ours, 0.03 ppb for the former and 0.26 ppb for the latter. Since the standard gas scales of CCGG and Tohoku were developed independently, the CCGG values were shifted upward by an average (0.15 ppb) of the two values in this study. The

latitudinal N_2O distribution deduced from the CCGG data is similar to ours, but there are some differences between both distributions; our values at 25° and 30°N (140°–150°E) in the western Pacific show N_2O concentrations higher by about 0.3 ppb than those at Sand Island, Midway (28°N, 177°W) and in the central Pacific Ocean (25°–30°N, 135°–139°W), whereas the CCGG values are higher by 0.1–0.5 ppb than our values between 10°N and 15°S, probably due to strong upwelling of N_2O-rich deep waters in the central and eastern tropical Pacific.

To examine the interannual variation of the N_2O concentration, we calculated the growth rates at the nine longitudes in the northern Pacific. The growth rates were also calculated for the latitudinal bands 55°–40°N, 35°–25°N, 20°–10°N, 5°N–5°S, 10°–20°S and 25°–40°S in the western Pacific, after the concentration data at the 20 latitude sites were grouped into these six latitudinal bands, on the basis of the average latitudinal distribution shown in Fig. 3. Area-weighted averages of the growth rates at these six latitudinal bands were then calculated to obtain Northern and Southern Hemispheric values. The growth rate for the latitudinal band of 5°N–5°S was included in the both hemispheric values in this procedure. The results are shown in Fig. 4, together with averages of the volumetric soil water content (SW) and the soil temperature (ST) at the depths of 0–10 and 10–200 cm (http://www.cdc.noaa.gov/cdc/data.reanalysis2.html), the sea surface temperatures (SST) (http://www.cdc.noaa.gov/cdc/data.noaa.ersst.html) and the multivariate El Niño Southern Oscillation (ENSO) index (MEI; http://www.cdc.noaa.gov/people/klaus.wolter/MEI/table.html) for the areas identified by the blue and red lines in Fig. 1, that is, 57.5°N–0° and 0°–42.5°S by 100°E–170°W, which are thought to affect the surface N_2O emissions.

The N_2O growth rates at all the locations show clear interannual variations with periods of about 3 yr, with a maximum growth for the period 1999–2000. In the northern Pacific, the growth rate variations appear to be different between the west side (150°E–180°E) and east side (170°W–130°W), with the east side lagging the west side by about 1 yr. This difference cannot be explained by the eastward transport of N_2O emitted in the Eurasia Continent, since zonal mixing time scale is shorter than 1 month. Therefore, differences in the oceanic N_2O emission and in the origin of air masses between the west and east sides could be responsible for such a phase delay. On the other hand, for the western Pacific, the N_2O growth rate in the low latitudes leads the one in the high latitudes, with a maximum phase difference of about 1.5 yr between the equator (5°N–5°S) and the northern highest latitude (55°–40°N). It is possible that this phase delay between the low and high latitudes is partly due to the poleward transport of N_2O emitted in the tropical region, but it is more likely that the interannual variations of local N_2O emissions and atmospheric transport effects (including stratospheric air intrusion) are responsible for the latitudinally different behaviour of the N_2O growth rate, as discussed in recent studies (Murayama et al., 2004; Nevison et al., 2007). Although many factors do influence the interannual variation of the atmospheric N_2O concentration, we investigate the impact of climate on surface N_2O emissions.

We consider two kinds of N_2O source for this area, that is, soils of natural and cultivated lands and oceans. SW/ST and SST are closely related to N_2O emissions from soils and oceans, respectively. Soil water content is one of the most important factors for N_2O emission from soils, and it can be used as an index indicating aerobic/anaerobic conditions that are indispensable for denitrification/nitrification by microbes since N_2O is produced and consumed by biochemical processes in soil. In terms of the soil physical property, SW is the most important factor in controlling the diffusivity of gaseous N_2O in soils. Soil water content can also be exploited as an index of nitrogen compounds supply from the atmosphere to soils via wet deposition. ST influences microbial activities producing/consuming N_2O and has some impact on the N_2O diffusivity in soil. SST is used as a measure of upwelling of N_2O-rich water, as well as of microbial activities and N_2O solubility in the surface ocean. The Southern Oscillation Index (SOI), which is substituted by MEI in this paper, is useful for discussing the relationship between the ENSO-related climate change and the atmospheric N_2O variation.

As seen in Fig. 4, all the climate parameters show interannual variations with periods of a few years in both hemispheres, in a similar fashion to the N_2O growth rate. The SW value increases rapidly around 2000, which is almost the same behaviour as the N_2O growth rate, suggesting that soil water plays an important role in the emission of N_2O from lands; in this case, the variations in the N_2O growth rate and SW occur in the Southern Hemisphere, before being observed in the Northern Hemisphere.

To examine the relative influence of the climate parameters on the N_2O growth rate, we performed a correlation analysis. The results are summarized in Table 1. The SW and SST correlate positively with the N_2O growth rate, whereas ST and MEI show a negative correlation. The correlation coefficients are higher in the Northern Hemisphere than in the Southern Hemisphere, implying that the Northern Hemispheric N_2O emissions are more influenced by climate conditions than in the Southern Hemisphere. The SW shows higher correlation with N_2O, on average, than ST and SST do, suggesting that soil water has primary effect on the interannual N_2O variation in our observation areas through its impact on the terrestrial N_2O emission. It is known that the variation of N_2O emission from land surface is significantly influenced by SW, although the fundamental productivity of N_2O depends on the local soil property such as texture and biochemical condition. It is possible that SW and precipitation affect N_2O emissions through microbial activities, as well as through processes such as the nitrogen deposition and freezing—thawing, especially in mid high latitudes, as shown by some recent studies (Pilegaard et al., 2006; Yu et al., 2007). The respective correlation coefficients of about 0.50 and –0.59 for SW and ST in the Northern Hemisphere may imply that high STs lead to low SWs.

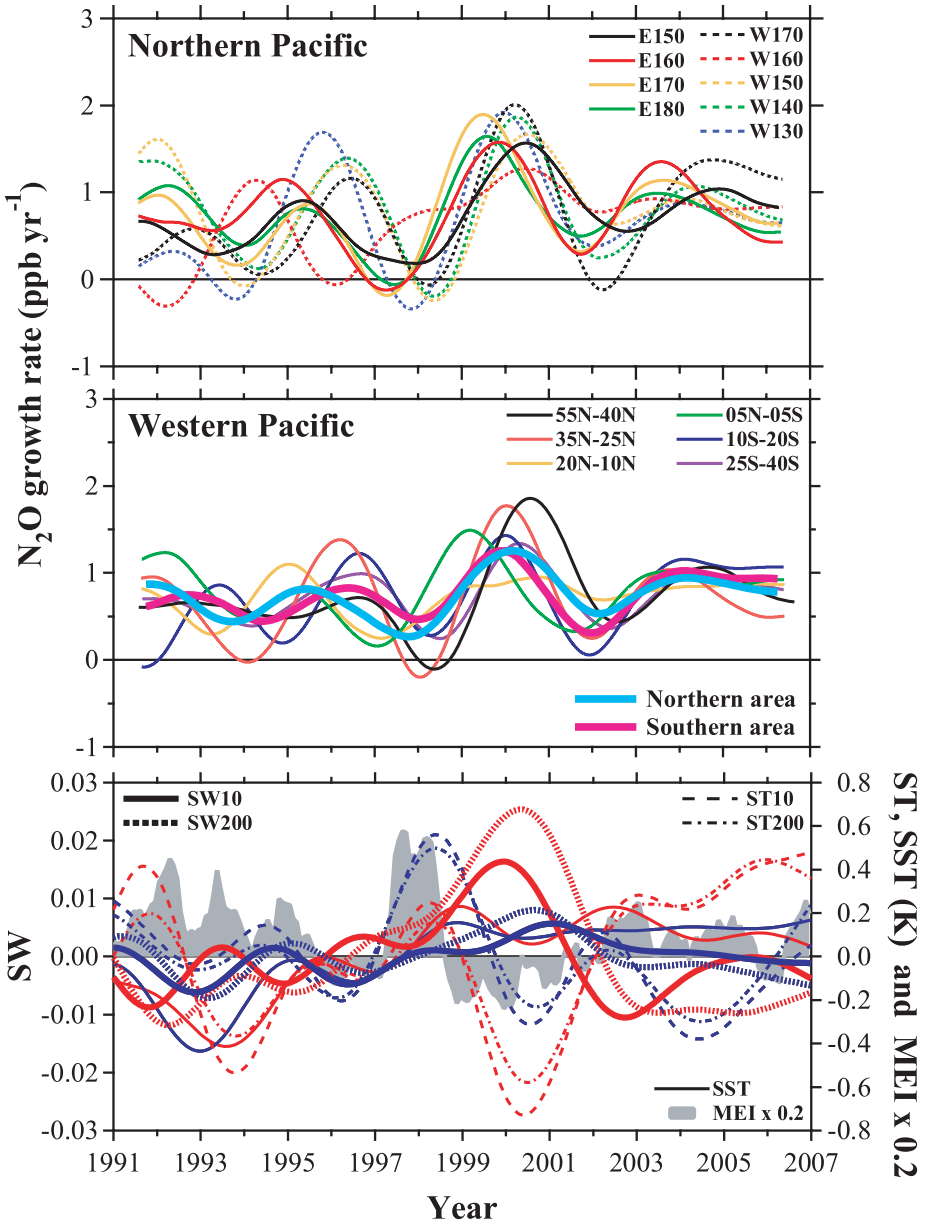

Fig. 4. Growth rates of the N_2O concentration at designated longitudes in the northern Pacific (upper) and at designated latitude intervals in the western Pacific (middle), and temporal variations of the volumetric soil water content (SW) and the soil temperature (ST) at 0–10 and 10–200 cm depths, the sea surface temperatures (SST) for both hemispheric areas (see Fig. 1) and the multivariate ENSO index multiplied by 0.2 (MEI x 0.2) (bottom). The N_2O growth rates for the northern and southern areas (see Fig. 1), weighed by the respective areas, are also shown in the middle panel. The interannual variations of the climate parameters were derived by applying the same digital-filtering technique that was used for the N_2O concentration. Red and blue lines represent the values for the northern and southern areas, respectively.

The correlation with the N_2O growth rate is clearly better for MEI than for SST, suggesting that the N_2O emission in the study region of the Pacific Ocean is influenced by ENSO events, probably in association with weakened upwelling of the N_2O-rich water from the deep ocean (Butler et al., 1989; Lueker et al., 2003; Nevison et al., 2005). It is also reasonable to conclude that tropical soils contribute to N_2O emissions through ENSO-related climate changes. Furthermore, ENSO-related changes in the atmospheric transport would be one of the important causal factors for the variations of atmospheric N_2O (Elkins et al., 1993; Ishijima et al., 2001). The interannual variation in the atmospheric N_2O concentration in the Southern Hemisphere reflects changes in the Northern Hemispheric N_2O emissions, as well as in the interhemispheric air exchange.

Table 1. Correlation coefficients of the N_2O growth rate with the volumetric soil water content (SW), the soil temperature (ST), the sea surface temperature (SST) and the multivariate ENSO index (MEI) for both hemispheres

	SW	ST	SST	MEI
Northern Hemisphere	0.502	−0.586	0.396	−0.517
Southern Hemisphere	0.337	−0.015	0.194	−0.437

Note: SW and ST are averages of values obtained at 0–10 and 10–200 cm depths.

With respect to the atmospheric transport effect, it may be worth describing an intrusion of the N_2O-poor stratospheric air into the troposphere. Only the N_2O concentration data obtained at 55°–40°N (grouped data in Fig. 4) using the new GC system showed a clear seasonal cycle with the seasonal maximum and minimum in spring and in summer to autumn, respectively. This finding agrees with the results obtained by previous studies (Liao et al., 2004; Nevison et al., 2004, 2007; Jiang et al., 2007), which reported a similar seasonal cycle at northern high latitudes. If the seasonal minimum is caused by the stratospheric air, as discussed in their papers, the interannual variation of tropospheric N_2O at northern high latitudes would also be closely related to the stratospheric air intrusion. Actually, Nevison et al. (2007) tried to explain the enhanced N_2O increase in 2000 in terms of the decreased intrusion of the N_2O-poor stratospheric air due to weakening of the mean meridional stratospheric circulation, although our results indicate the possibility that the N_2O concentration increase was partly due to some soil emission changes.

5. Conclusions

The atmospheric N_2O concentration was observed in the northern and western Pacific for the period 1991–2005, using commercial container ships sailing between Japan and North America and between Japan and Australia or New Zealand. The N_2O concentration showed an increasing secular trend and interannual variations at all sampling locations. The seasonal N_2O cycle with maximum in spring and minimum in summer to autumn was detectable only at northern high latitudes by using a high-precision GC system. The annual mean N_2O concentration was nearly independent of the longitude in the northern Pacific due to the zonally well-mixed atmosphere, as well as a lack of any strong sources/sinks in this area. On the other hand, the annual mean N_2O concentration showed a clear north-south gradient, the Northern Hemispheric values being higher by 0.8 ppb, on average, than the Southern Hemispheric values, suggesting that the N_2O emission is stronger in the Northern Hemisphere than in the Southern Hemisphere, mainly due to N_2O emissions from soils. The latitudinal N_2O distribution showed high values around 30°N due to local N_2O emissions, as well as a steep gradient from the equator to 20°S due to the suppression of the southward transport of the Northern Hemispheric air by the SPCZ. It was also observed that the growth rate of the N_2O concentration varied interannually with periods of about 3 yr, with notable high values during the period 1999–2000. The interannual variation of the growth rate displayed phase delays in its propagation eastward and poleward in the northern and western Pacific, respectively. By examining the correlations of the interannual variation of the N_2O growth rate with those of some climate parameters, we found that soil water showed the highest correlation coefficient in both hemispheres. The MEI varied in almost opposite phase with the N_2O growth rate in both hemispheres, which suggests that the ENSO-related changes in the oceanic N_2O emission and atmospheric transport are also important for the interannual variation of the atmospheric N_2O concentration.

For a better understanding of the temporal and spatial variations of atmospheric N_2O, its concentration measurements using such high precision analytical instruments as our new GC system need to continue. High precision measurements of the isotopic ratios of N_2O would also be crucial, especially for examining N_2O emissions from natural and anthropogenic sources and its destruction in the stratosphere. Numerical analyses using global atmospheric transport models with N_2O source/sink processes are further needed to interpret the atmospheric N_2O variation in detail.

6. Acknowledgments

We express our gratitude to the staff of the container ships, M/S California Orion, NYK Starlight, NYK Altair, NYK Procyon, NYK Rodestar, NYK Springtide, Nichigo-maru, AOTEA and M.V. HAKONE, for their cooperation in collecting air samples.

We also deeply thank Dr Ed Dlugokencky, NOAA/ESRL/GMD/CCGG, for allowing us to use their unpublished data in this paper. This study was partly supported by the Grants-in-Aid for Creative Scientific Research (2005/17GS0203) of the Ministry of Education, Science, Sports and Culture, Japan.

References

Bouwman, A. F. and Taylor, J. A. 1996. Testing high-resolution nitrous oxide emission estimates against observations using an atmospheric transport model. *Global Biogeochem. Cycles* **10**, 307–318.

Butler, J. M., Elkins, J. W. and Thompson, T. M. 1989. Tropospheric and dissolved N_2O of the west Pacific and east Indian Oceans during the El Niño-Southern Oscillation event of 1987. *J. Geophys. Res.* **94**, 14865–14877.

Ehhalt, D., Prather, M., Dentener, F., Derwent, R., Dlugokencky, E. and co-authors. 2001. Atmospheric chemistry and greenhouse gases. In:

Climate Change 2001: The Scientific Basis (eds. J. T. Houghton, and co-editors). Cambridge University Press, New York, 239–287.

Elkins, J. W., Thompson, T. M., Swanson, T. H., Butler, J. H., Hall, B. D. and co-authors. 1993. Decrease in the growth rates of atmospheric chlorofluorocarbons 11 and 12. *Nature* **364**, 780–783.

Flückiger, J., Dällenbach, A., Blunier, T., Stauffer, B., Stocker, T. F. and co-authors. 1999. Variations in atmospheric N_2O concentration during abrupt climatic changes. *Science* **285**, 227–230.

Forster, P., Ramaswamy, V., Artaxo, P., Berntsen, T., Betts, R. and co-authors. 2007. Changes in Atmospheric Constituents and in Radiative Forcing. In: *Climate Change 2007*: *The Physical Science Basis. Contribution of Working Group I to the Fourth Assessment Report of the Intergovernmental Panel on Climate Change*. Cambridge University Press, Cambridge, United Kingdom and New York, NY, USA.

Gloor, M., Fan, S., Pacala, S. and Sarmiento, J. 2000. Optimal sampling of the atmosphere for purpose of inverse modeling: a model study. *Global Biogeochem. Cycles* **14**, 407–428.

Hofmann, D. J., Butler, J. H., Dlugokencky, E. J., Elkins, J. W., Masarie, K. and co-authors. 2006. The role of carbon dioxide in climate forcing from 1979 to 2004: introduction of the Annual Greenhouse Gas Index. *Tellus* **58B**, 614–619.

Hirsch, A. I., Michalak, A. M., Bruhwiler, L. M., Peters, W., Dlugokencky, E. J. and co-authors. 2006. Inverse modeling estimates of the global nitrous oxide surface flux from 1998–2001. *Global Biogeochem. Cycles* **20**, GB1008, doi:10.1029/2004GB002443.

Ishijima, K., Nakazawa, T., Sugawara, S., Aoki, S. and Saeki, T. 2001. Concentration variations of tropospheric nitrous oxide over Japan. *Geophys. Res. Lett.* **28**, 171–174.

Ishijima, K., Sugawara, S., Kawamura, K., Hashida, G., Morimoto, S. and co-authors. 2007. Temporal variations of the atmospheric nitrous oxide concentration and its $d^{15}N$ and $d^{18}O$ for the latter half of the 20th century reconstructed from firn air analyses. *J. Geophys. Res.* **112**, 3305, doi:10.1029/2006JD007208.

Jiang, X., Ku, W. L., Shia, R. L., Li, Q., Elkins, J. W. and co-authors. 2007. Seasonal cycle of N_2O: analysis of data. *Global Biogeochem. Cycles* **21**, GB1006, doi:10.1029/2006GB002691.

Lueker, T. J., Walker, S. J., Vollmer, M. K., Keeling, R. F., Nevison, C. D. and co-authors. 2003. Coastal upwelling air-sea fluxes revealed in atmospheric observations of O_2/N_2, CO_2 and N_2O. *Geophys. Res. Lett.* **30**, 1292, doi:10.1029/2002GL016615.

Liao, T., Camp, C. D. and Yung, Y. L. 2004. The seasonal cycle of N_2O. *Geophys. Res. Lett.* **31**, L17108, doi:10.1029/2004GL020345.

MacFarling Meure, C., Etheridge, D., Trudinger, C., Steele, P., Langenfelds, R. and co-authors. 2006. Law Dome CO_2, CH_4 and N_2O ice core records extended to 2000 years BP. *Geophys. Res. Lett.* **33**, 14810, doi:10.1029/2006GL026152.

Machida, T., Nakazawa, T., Fujii, Y., Aoki, S. and Watanabe, O. 1995. Increase in the atmospheric nitrous oxide concentration during the last 250 years. *Geophys. Res. Lett.* 22, 2921–2924.

Mosier, A., Kroeze, C., Nevison, C., Oenema, O., Seitzinger, S. and co-authors. 1998. Closing the global N_2O budget: nitrous oxide emissions through the agricultural nitrogen cycle. *Nutrient Cycling Agroecosyst.* **52**, 225–248.

Murayama, S., Taguchi, S. and Higuchi, K. 2004. Interannual variation in the atmospheric CO_2 growth rate: Role of atmospheric transport in the Northern Hemisphere. *J. Geophys. Res.* **109**, D02305.

Nakazawa, T., Ishizawa, M., Higuchi, K. and Trivett, N. B. A. 1997. Two curve fitting methods applied to CO_2 flask data. *Environmetrics* **8**, 197–218.

Nevison, C. D., Weiss, R. F. and Erickson, D. J., III. 1995. Global oceanic emissions of nitrous oxide. *J. Geophys. Res.* **100**, 15 809–15 820.

Nevison, C. D., Kinnison, D. E. and Weiss, R. F. 2004. Stratospheric influences on the tropospheric seasonal cycles of nitrous oxide and chlorofluorocarbons. *Geophys. Res. Lett.* **31**, L20103, doi:10.1029/2004GL020398.

Nevison, C. D., Keeling, R.F., Weiss, R. F., Popp, B. N., Jin, X. and co-authors. 2005. Southern Ocean ventilation inferred from seasonal cycles of atmospheric N_2O and O_2/N_2 at Cape Grim, Tasmania. *Tellus* **57B**, 218–229.

Nevison, C. D., Mahowald, N., Weiss, R. F. and Prinn, R. G. 2007. Interannual and seasonal variability in atmospheric N_2O. *Global Biogeochem. Cycles* **21**, doi:10.1029/2006GB002755.

Patra, P. K., Maksyutov, S., Baker, D., Bousquet, P., Bruhwiler, L. and co-authors. 2003. Sensitivity of optimal extension of observation networks to model transport. *Tellus* **55B**, 498–511.

Pilegaard, K., Skiba, U., Ambus, P., Beier, C., Brüggemann, N. and co-authors. 2006. Factors controlling regional differences in forest soil emission of nitrogen oxides (NO and N_2O). *Biogeosciences* **3**, 651—661.

Prinn, R. G., Weiss, R. F., Fraser, P. J., Simmonds, P. G., Cunnold, D. M. and co-authors. 2000. A history of chemically and radiatively important gases in air deduced from ALE/GAGE/AGAGE. *J. Geophys. Res.* **105**, 17 751–17 792, doi:10.1029/2000JD900141.

Suntharalingam, P. and Sarmiento, J. L. 2000. Factors governing the oceanic nitrous oxide distribution: simulations with an ocean general circulation model. *Global Biogeochem. Cycles* **14**, 429–454, doi:10.1029/1999GB900032.

Weiss, R. F. 1981. The temporal and spatial distribution of tropospheric nitrous oxide. *J. Geophys. Res.* **86**, 7185–7195.

Yu, J., Sun, W., Liu, J., Wang, J., Yang, J. and co-authors. 2007. Enhanced net formations of nitrous oxide and methane underneath the frozen soil in Sanjiang wetland, northeastern China. *J. Geophys. Res.* **112**, D07111, doi:10.1029/2006JD008025.